A New Estimate of the Cutoff Value in the Bak-Sneppen Model

C. A. Fish[1], J. J. P. Veerman[2]

December 28, 2022

Abstract

We present evidence that the Bak-Sneppen model of evolution on N vertices requires N^3 iterates to reach the stationary state. This is substantially more than previous authors suggested (on the order of N^2). Based on that estimate, we present a novel algorithm inspired by previous rank-driven analyses of the model allowing for direct simulation of the model with populations of up to $N = 25600$ for $2 \cdot N^3$ iterations. These extensive simulations suggest a cutoff value of $x^* = 0.66747 \pm 0.00025$, a value slightly higher than previously estimated. We also study how the cutoff values x_N^* at finite N approximate the conjectured value x^* at $N = \infty$. Assuming $x_N^* - x_\infty^* \sim N^{-\nu}$, we find values of ν which are significantly lower than previous estimates.

We also present evidence supporting earlier conjectures that the bulk of the replacements in the Bak-Sneppen model occur in a decreasing fraction of the population as $N \to \infty$.

Keywords— Bak-Sneppen model, critical threshold, rank driven dynamical systems, discrete dynamical systems, self-organized criticality, one-dimensional cellular automata

1 Introduction

The Bak-Sneppen model (BS) is a discrete dynamical system defined as follows. Choose a population size $N \in \mathbb{N}$ and consider a cyclic graph with N nodes. Assign to each node a *fitness* value uniformly at random from $[0, 1] \subset \mathbb{R}$. Name these fitness values $(x_1, x_2, ...x_N)$ so that x_N and x_1 are neighbors (i.e. $x_{N+1} := x_1$ and $x_0 := x_N$). At each time step, determine the node x_j with smallest fitness (the *weakest*) and replace both it and its neighbors x_{j-1} and x_{j+1} with fresh values chosen uniformly at random from $[0, 1]$ (we say the minimum node has *mutated*).

Via this process, the weakest nodes are repeatedly eliminated in a way reminiscent of biological evolution. The mutation of nodes neighboring the weakest coarsely reflects the effects of disappearing species on nearby species. Bak and Sneppen in [1] suggest that this model has dynamic features also seen in biological evolution, namely "Self-organized criticality" (see also [4] for discussion of "punctuated equilibrium" and [2] for precise exploration of these features).

Observe that if the fitness of the weakest node x_j decreases in a mutation, then the new weakest is one of x_j, x_{j-1} or x_{j+1}. In any case x_j will mutate on the next time step. Thus there is an "upward pressure" counteracted by the fact that strong nodes are always at risk of being neighbors to the weakest. Indeed, it was shown in [10] that the mean of the (time) limiting distribution of fitnesses is bounded away from 1, as the population size $N \to \infty$ (see [14] for a survey of related results).

After an initial period during which the overall fitness increases, the model reaches a stationay state with the vast majority of the values above a certain *cutoff value*. Computer simulations suggest that, for each N, the (time) limiting distribution of fitnesses is uniform on $[x_N^*, 1]$ for some cutoff x_N^* depending on N. Moreover, it appears that as $N \to \infty$, the sequence of cutoff values x_N^* approaches a limiting value close to $2/3$. This cutoff value x^* has been experimentally estimated as 0.66702 ± 0.00008 [5], 0.66702 ± 0.00003 [13], and 0.6672 ± 0.0002 [3]. It was shown in [11] that, under certain assumptions, the cutoff is strictly less than 0.75.

[1]Fariborz Maseeh Department of Math and Statistics, Portland State University; cafish@pdx.edu

[2]Fariborz Maseeh Department of Math and Statistics, Portland State University; veerman@pdx.edu

We found that on the order of N^3 time steps are required to reach the stationary state (see Figure 2 and Table 1). Since at each timestep the weakest node must be found (which naively takes $O(N)$ time), the overall naive runtime is $O(N^4)$. Thus it is computationally intensive to estimate the cutoff using naive iteration of the model. Because the model doesn't lend itself to parallelization, it is difficult to find a quicker way to run reliable simulations. Indeed, prior literature has focused on finding models which are less intensive to simulate and give the same exponents and cutoff. In particular, [5] and [13] study the "BS branching process" in which the system is initialized with conditions close to the stationary state, and statistical properties of the avalanches are measured. These properties, together with an assumption about the scaling behavior of the avalanches, allow for an estimation of the cutoff. In the interest of supporting these results, we have made use of certain characteristics of the "rank dynamics" of the model to efficiently perform a direct simulation, making no assumptions about the scaling behavior. Our simulations of the model are the largest to date: namely $2 \cdot N^3$ time steps for $N = 25600$. In comparison, Garcia et al. [3] simulated $N = 8000$ for only $O(N^2)$ time steps.

By simulating the model directly, we obtain empirical fitness distributions in which the cutoff can be "seen" clearly (see Figure 2). Since it is not immediately clear how to best estimate the cutoff from this data, we employed three different methods to obtain a range of possible values. Firstly ("Method 1"), we take the first index at which the value of the histogram is above a threshold. This method is expected to underestimate the cutoff (due to always taking the leftmost index), and indeed gives an estimate $x^* = 0.66688 \pm 0.00004$. Secondly ("Method 2"), we measure the heights of the histograms, making use of the fact that the fitness distribution approaches uniform on $(x^*, 1)$ as $N \to \infty$, arriving at $x^* = 0.66717 \pm 0.00010$. Finally ("Method 3"), we model the distribution of fitness values with a density function ρ_N having parameters that scale with N. This method takes into account information about the entire shape of the fitness distribution (rather than a single measurement, as in our other two methods). Via this method, we estimated a value of $x^* = 0.66747 \pm 0.00025$, a value slightly (but significantly) higher than previously estimated.

In addition, we studied how the cutoff values x_N^* at finite N approximate the conjectured value x^* at $N = \infty$. Assuming $x_N^* - x_\infty^* \sim N^{-\nu}$, we find that $\nu = 0.717 \pm 0.027$ (via Method 3), $\nu = 0.728 \pm 0.017$ (via Method 2), or $\nu = 0.978 \pm 0.024$ (via Method 1), all of which are significantly lower than previous estimates (e.g. [3] gives $\nu \approx 1.4$).

2 Dynamical Characteristics of the Model

2.1 *Onset of the stationary state*

Our approach is to iterate the model T_N times on N nodes until it reaches the stationary state. Once it does, we iterate it another T_N times during which we perform our measurements. This way we insure that measurements are taken while the system is in the stationary state. Figure 2 provides evidence that the stationary state sets in after approximately $T_N = N^3$ iterates of the system. We found similar behavior for other values of N.

We emphasize that this analysis is only meant to suggest the approximate number of iterations required to reach the stationary state. We will later demonstrate a more robust method of fitting these fitness distributions to a density function.

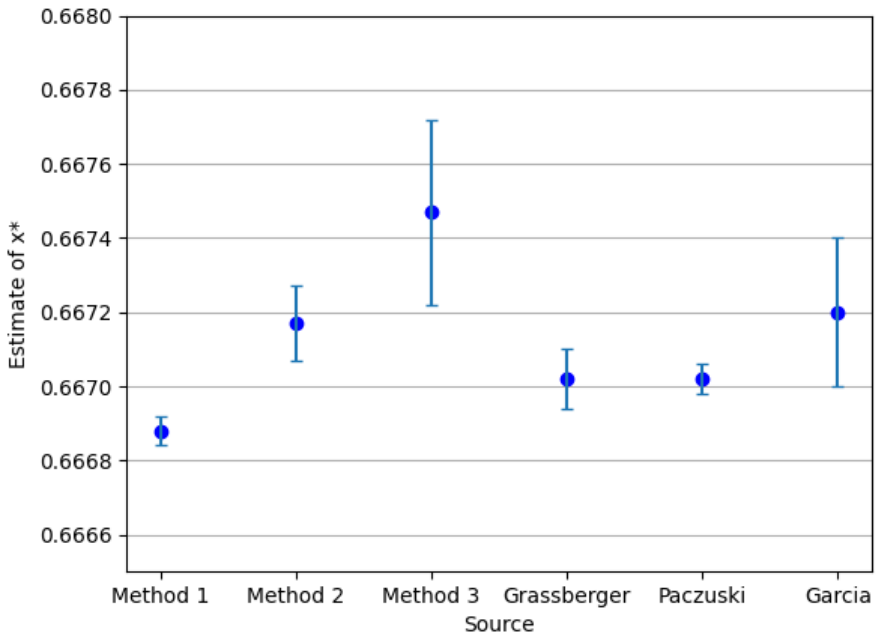

Figure 1: Comparison of our estimated cutoff values and those estimated by Grassberger [5], Paczuski [13], and Garcia [3]. As detailed in Section 4, we used three separate methods to obtain the cutoff values shown.

2.2 *Most Replacements Have Low Rank*

We can order the values of the fitness distribution by their *rank*. The lowest fitness is ranked "1", the next lowest gets rank "2", et cetera. The rank-driven analysis put forward in [6], [7], and [14] strongly suggests that the vast majority of mutations occur at the lowest ranks. For example, Figure 3 illustrates the frequency at which the different ranks are replaced (after reaching the stationary distribution) for one simulation at $N = 800$. The overwhelming majority of replacements occur below rank 50. This motivates maintaining a "short list" containing only the lowest-ranked nodes. Mutated nodes may enter and leave the short list, where they stay "waiting" to be mutated. If the list grows too small, it is rebuilt by sorting the entire population. Keeping track only of relatively few lowest-ranked nodes on the short list allows us to find the position of the lowest ranked node without searching the whole population. The trick is to keep the list long enough so that we avoid sorting the entire population too often. This strategy allows us to iterate the model $2 \cdot N^3$ times in approximately $O(N^3 \log N)$ time (compare the naive method at $O(N^4)$ and a standard heap method at $O(N^3 \log N)$ as discussed in Section 3.1).

2.3 *High Rank Replaced at Constant Rate*

The rank-driven approach of [14] implies that the cutoff can be precisely determined if the sequence (indexed by the population size N) of sequences (indexed by rank i) of rank replacement frequencies $\{\alpha_i(N)\}_{i=1}^{N}$ form a so-called (p, q)-array. This is an array $\{\alpha_i(N)\}_{i=1}^{N}$ such that there exist p, q independent of N with

$$\sum_{i=0}^{K(N)} \alpha_i \le p < \sum_{i=1}^{K(N)+1} \alpha_i \quad \text{and} \quad q = \sum_{i=1}^{N} \alpha_i \,.$$

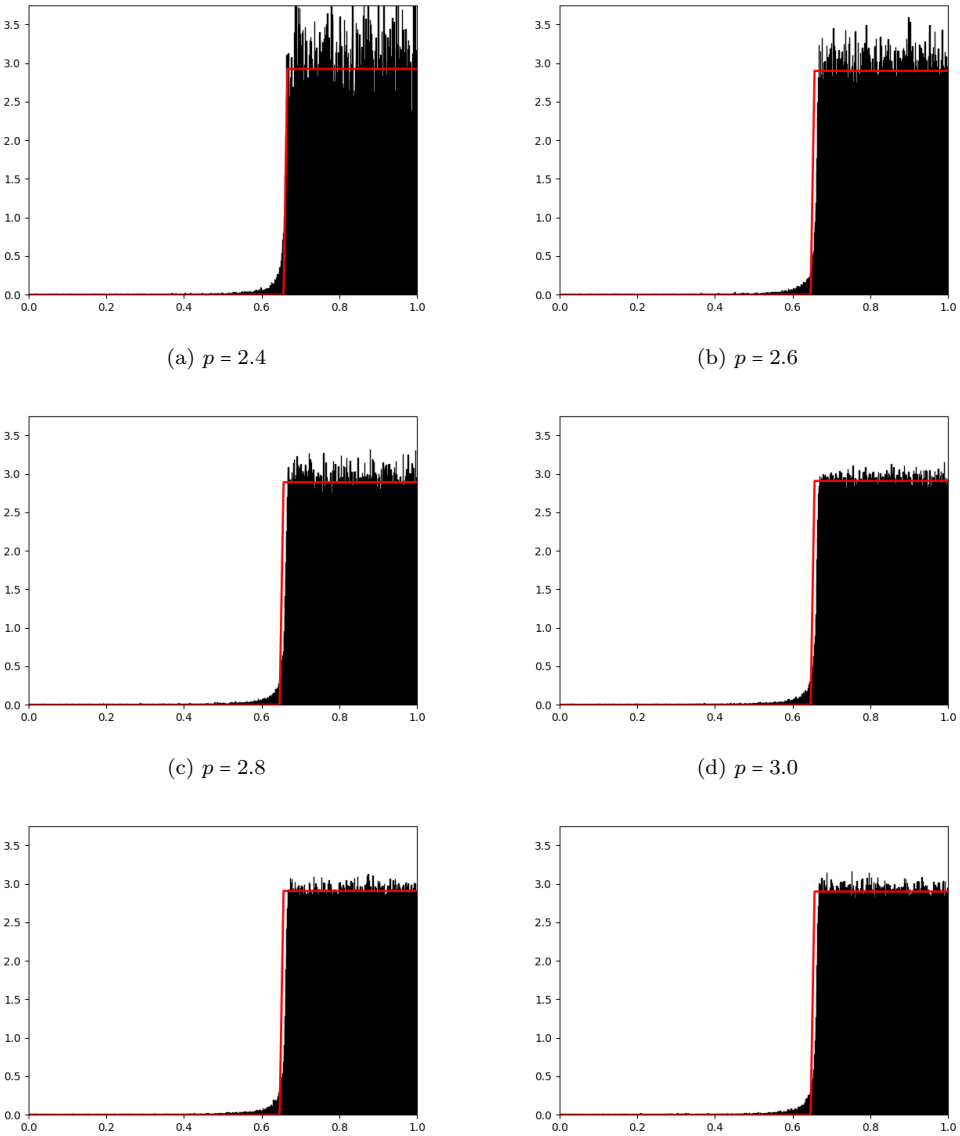

(a) $p = 2.4$ (b) $p = 2.6$

(c) $p = 2.8$ (d) $p = 3.0$

(e) $p = 3.2$ (f) $p = 3.4$

Figure 2: Histograms of fitness values for 500 population samples made after N^p time steps, for $N = 800$ and for $p \in \{2.4, 2.6, 2.8, 3.0, 3.2, 3.4\}$. These data suggest that the stationary state is reached at $p \approx 3$. The uniform distribution on $(x^*, 1)$ has been overlaid, for x^* determined individually for each histogram (by Method 2, described below). In Table 1 we report the Cramér-von Mises and Kolmogorov-Smirnov statistics for these data.

p	x^*	C.V.M. statistic	Kolmogorov-Smirnov statistic
2.4	0.658	8.325	0.0186
2.6	0.655	1.293	0.0160
2.8	0.654	0.915	0.0154
3.0	0.656	1.043	0.0164
3.2	0.656	1.001	0.0162
3.4	0.655	0.855	0.0155

Table 1: We computed the Cramér-von Mises and Kolmogorov-Smirnov statistics (see e.g. [12]) on the empirical distribution of fitness values sampled 500 times after N^p time steps, for $N = 800$. The statistic gives a measure of distance between the empirical distribution of the sample and the uniform distribution on $(x^*, 1)$. As seen, the CVM statistic is somewhat larger for $p \in \{2.4, 2.6\}$ but is more consistent for higher values, suggesting that at least $p \approx 2.8$ is needed.

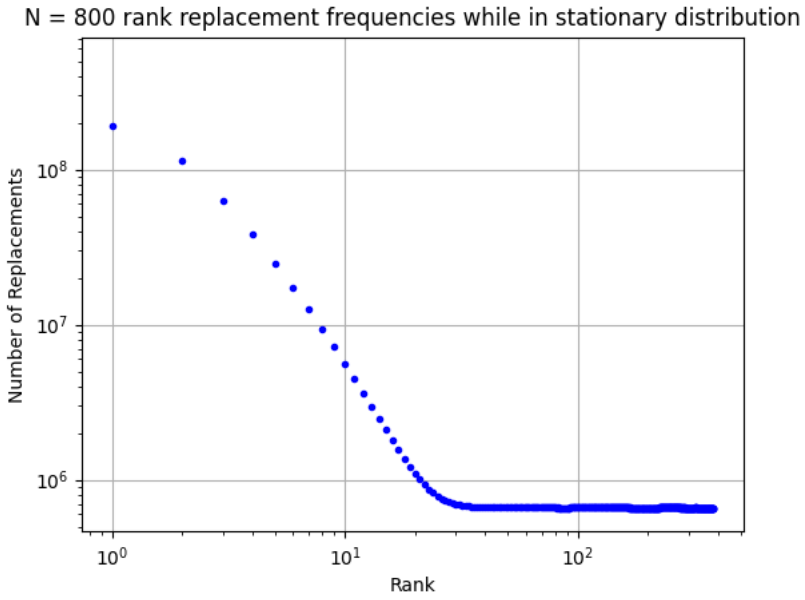

Figure 3: The frequency of mutation by rank found in one execution of the Bak-Sneppen model at $N = 800$. The minimum node (rank 0) is replaced the most often (since it is mutated every time step), and it appears that all but the lowest-ranked nodes are mutated rarely and at roughly equal frequency. (Note the logarithmic axes.)

for some $K(N) \in (1, N)$ depending on N such that $K(N) = o(N/\ln N)$. Furthermore, there must exist $\delta_i(N)$ and $\tilde{\alpha}(N)$ depending on N such that for ranks $i > K(N)$, the rank replacement frequencies α_i take the form $\tilde{\alpha}(N) + \delta_i(N)$ where $\max_{i>K(N)} |\delta_i(N)| = o(1/N)$ and $\tilde{\alpha}(N)$ is a constant – that is, the tail of the sequence of $\alpha_i(N)$ should increasingly flat as N tends to infinity. If the replacements frequencies $\{\alpha_i(N)\}$ form a (p, q) array, then one can prove [14] that the cutoff equals $\frac{p}{q}$.

Our data are consistent with the hypothesis that the sequences $\{\alpha_i(N)\}_{i=1}^{N}$ form a (p, q)-array, as illustrated in Figure 4. A more rigorous check is difficult in practice since the precise criterion for selecting $K(N)$ from data alone is unclear, and small errors in that choice amount to large differences in the estimate of x^*. Further investigation would indeed be useful.

2.4 *Continuity of High Rank Replacement Rate*

We also observe an unexpected continuity in the rank replacement frequencies (as in Figure 4); rank neighbors have correlated replacement frequencies. We propose the following heuristic explanation, making use of the fact that the distribution, $C(x)$, of the distance x between subsequent mutations is known (e.g. [1]) to follow a power law $C(x) = x^{-3.15\pm0.05}$. Let $R_t(x_i)$ be the rank of node x_i at time t, and let $P_t(r)$ be the probability that the node with rank r is mutated at time t. Suppose that at time t the least-fit node is x_m, and so will mutate next. Consider some node x_k, distinct from x_m, x_{m-1}, and x_{m+1}. Prior to mutation, there is an approximate chance $p = C(d(x_m, x_k))$ that x_k will be mutated next[3]. Since x_k has rank $R_t(x_k)$, we can say $P_t(R_t(x_k))$ is also approximately p. After the mutation, at time $t+1$, the new minimum is likely[4] to be one of x_m, x_{m-1}, or x_{m+1}. If so, the chance that x_k is mutated next will be close to p, by the continuity of $C(x)$. Hence $P_{t+1}(R_{t+1}(x_k))$ is also close to p. However, $R_{t+1}(x_k)$ may differ from $R_t(x_k)$ due to the mutation, by at most 3. Thus, for

[3]The value $d(x_m, x_k)$ being the minimal distance between x_m and x_k, i.e. the minimum of $|m-k|$ and $N-|m-k|$.
[4]The new minumum must be one of these three nodes unless all three increase in fitness as a result of the mutation.

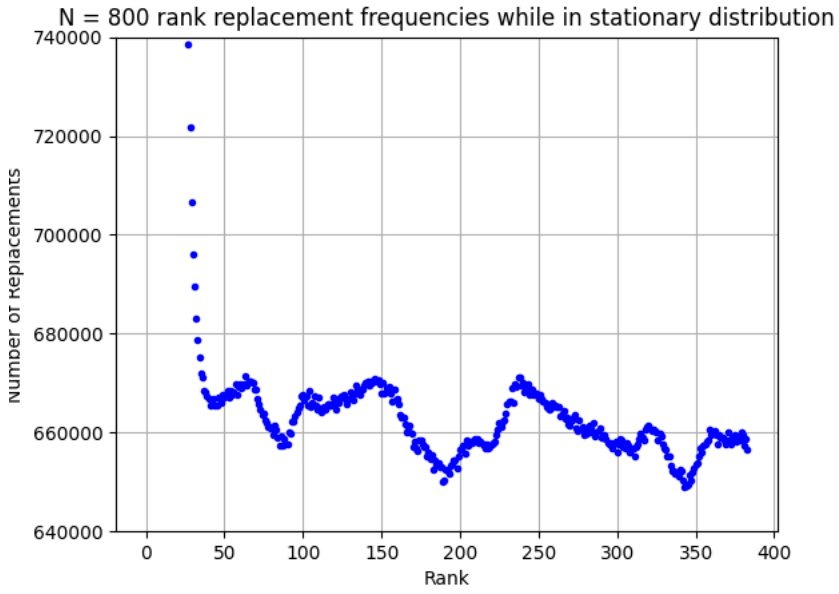

Figure 4: The frequency of mutation by rank found in one execution of the Bak-Sneppen model at $N = 800$, displaying only the vertical range $[640000, 740000]$. The data are very close to flat: the frequency beyond rank 50 deviates from flat by less than 2 out of 66 or ±1.5%. Observe also that replacement rates appear to be continuous, perhaps even smooth (rather than random deviations from a mean).

$r = R_t(x_k) \pm 3$, we have $P_{t+1}(r) \approx P_t(R_t(x_k)) \approx p$, leading to an apparent approximate continuity in the graph of rank replacement frequencies.

3 Simulation Method

To simulate the model with our "short list" method, we used a multi-linked-list data structure to keep track of the fitnesses, their *position neighbors*, and possibly their *rank neighbors*. That is, to represent the fitness value x_j, we create a node containing:

- a `double`[5] approximating x_j
- a pointer to the node with fitness x_{j-1}
- a pointer to the node with fitness x_{j+1}
- (possibly) a pointer to the node with next largest fitness
- (possibly) a pointer to the node with next smallest fitness

Choosing some k depending on N, the simulation is initialized with only the $5k$ lowest-ranked nodes having pointers to their rank-neighbors. We also maintain pointers to the lowest and highest values on the short list.

To update the simulation once, the fitness of the lowest-ranked node x_j is replaced, along with the fitnesses of its two position neighbors x_{j-1} and x_{j+1}. It is then determined, for each of the three

[5] a 64-bit floating-point type; see [8] for details

nodes x_j, x_{j-1}, x_{j+1}, whether they should or should not be on the short list. This is easy to check by comparing a new fitness value with the fitness of the highest-ranked node on the short list: the new fitness should be on the short list only if it is strictly less than this highest-ranked value. The neighbors x_{j-1} and x_{j+1} may or may not be on the short list already, and so may remain on, remain off, be inserted, or be removed. The rankings of all members of the short list are maintained appropriately as these operations are performed. If the length of the short list ever increases above $5k$, the ranks above $5k$ are simply "forgotten". If it decreases to below $3k$, it is rebuilt by sorting the population. This last operation is expensive, but occurs infrequently (for example, in one simulation of 800 nodes lasting $800^3 = 5.12 \times 10^8$ iterations, the short list was rebuilt only 1419 times; see also Figure 5).

This method allows for simulation of large population values in a reasonable time. Our longest simulations ($N = 25600$) required approximately 45 days to complete[6], while carrying out the same simulation using the naive method would take an estimated several thousand days.

Both the speed of the simulation and the frequency at which the short list is rebuilt will depend on the choice of k. We chose $k = 8$ for $N \in \{100, 200, 400\}$, $k = 16$ for $N \in \{800, 1600, 3200\}$, $k = 24$ for $N \in \{6400, 12800\}$, and $k = 32$ for $N = 25600$. These choices are likely not optimal and merit further investigation.

3.1 *Runtime analysis*

At a given point in time, let x_{min} denote the minumum node and x_{smax} denote the largest node on the short list. In a single interation of the algorithm, the following steps are performed:

(1) Determine x_{min} and its position neighbors. Then generate three new random values. For each new value, determine if it is less than x_{smax}

(2) If a new value is less than x_{smax}, perform a walk through the shortlist to determine its new rank.

(3) Determine if the shortlist needs to be rebuilt by checking if its length is below $3k$. If so, then sort the population and repopulate the shortlist.

Step (1) is $O(1)$ since pointers to x_{min} and x_{smax} are maintained.

Step (2) is $O(k)$ if it occurs, since the maximum length of the shortlist is $5k$. The probability that a new value is less than x_{smax} is just $x_{smax} < 1$, because it is chosen uniformly at random in $(0, 1)$. One may attempt to determine the average value of x_{smax}, but since this average is no more than 1, step (2) is $O(k)$ regardless.

Step (3) is $O(k + N \log N)$ if it occurs, since the population is first sorted with a standard efficient algorithm, and then the shortlist of length $O(k)$ is repopulated. Let R be the probability that this occurs.

Thus, a single iteration of the algorithm is on average $O(k + R(k + N \log N))$. Although a theoretical value of R is difficult to determine, an empirical estimate can be found by tracking how often the shortlist is rebuilt (see Table 2).

If we assume that the probability R grows as $O(N^{-2})$ (see Figure 5), then a single iteration of the algorithm becomes $O(k + N^{-2}k + N^{-1} \log N)$. In our simulations, the value of k was chosen depending on N (see Figure 6). With these choices, k grows roughly as $O(\log N)$. If we assume $k = O(\log N)$, then

[6] on the Coeus HPC Cluster provided through the Portland Institute for Computational Science and Portland State University

N	Mean number of occurrences	Estimated R
100	54.200	$2.710 \cdot 10^{-5}$
200	79.600	$4.975 \cdot 10^{-6}$
400	325.375	$2.542 \cdot 10^{-6}$
800	1423.175	$1.390 \cdot 10^{-6}$
1600	7073.000	$8.634 \cdot 10^{-7}$
3200	41310.925	$6.304 \cdot 10^{-7}$
6400	276566.175	$5.275 \cdot 10^{-7}$
12800	2023577.800	$4.825 \cdot 10^{-7}$
25600	2267531.579	$6.758 \cdot 10^{-8}$

Table 2: For each population value, the number of times the shortlist was rebuilt was recorded and averaged over all runs. Dividing by the total iterations $2N^3$ gives an estimate for R, the probability that the shortlist is rebuilt.

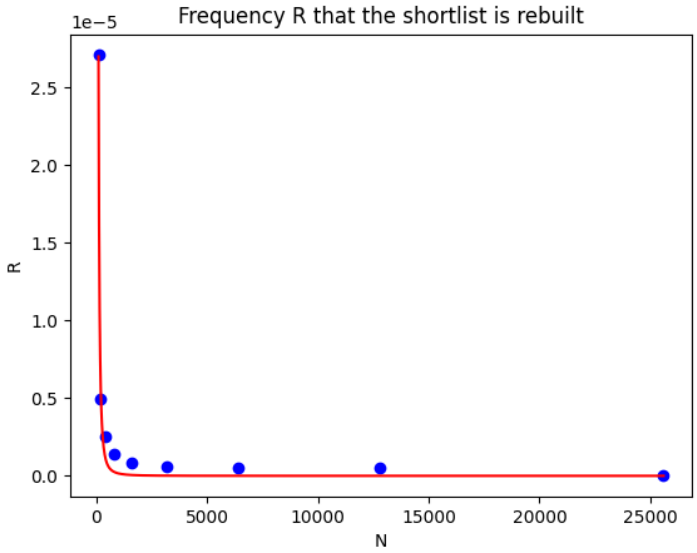

Figure 5: Empirical estimate of R, the probability that the shortlist is rebuilt on a given iteration of the algorithm. The fitted curve is given by $R(N) = 0.805N^{-2.24}$, giving a growth rate of approximately $O(N^{-2})$.

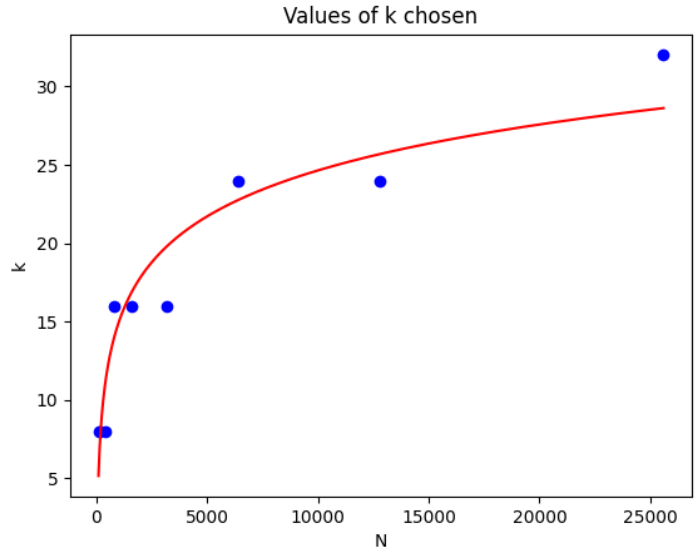

Figure 6: The values of k chosen for our simulations grow as approximately $O(\log N)$. The fitted curve shown is $k(N) = 9.74 \log_{10}(N) - 14.33$. The optimal values of k merit further investigation.

our average runtime for a single step becomes $O(\log N + N^{-2}\log N + N^{-1}\log N)$ i.e. $O(\log N)$. This is comparable with a standard heap-based algorithm (e.g. [5]) which takes $O(\log N)$ time to perform a single iteration. This runtime may be futher reduced by more accurately selecting k.

4 Estimation of the Cutoff

4.1 *The cutoff for finite* N

To estimate the cutoff value x_N^* for finite N, we performed simulations for various population values, using two separate pseudorandom number generators (RNGs) in order to mitigate bias: `xoshiro256+` ("Xoshiro", see [15]) and `MT19937-64` ("Mersenne twister", see [9]). For each RNG we performed 20 simultaneous executions of the model at each of the population levels $N = 100 \cdot 2^i$ for $i \in \{0, ..., 8\}$.

In each execution, we first iterate N^3 times to reach the stationary state. Then, iterate N^3 times during which 500 snapshots are taken: one after each $N^3/500$ iterates. Collect these data into a histogram, in which the cutoff value is distinctly visible (see Figure 7). Using these histograms, we estimate the cutoff x^* in three different ways. The raw cutoff data for Methods 1 and 2 is summarized in Table 3. We also report "combined" values by pooling data from both RNGs before taking the mean and standard deviation.

4.1.1 Method 1

Since we expect the limiting fitness distribution

$$f(x) = \begin{cases} 0 & 0 \le x < x^* \\ \frac{1}{1-x^*} & x^* \le x \le 1 \end{cases},$$

with $x^* \approx 2/3$, it is reasonable to define the transition point as the first index in the histogram at which the height exceeds a threshold $T = 1.5$.

Since we we expect a discontinuity at x^* in the limiting distribution, any choice of $T \in (0, 1)$ should (eventually) provide an identical cutoff value, and the choice of 1.5 is for convenience. As Figure 8 illustrates, the estimate of x^* is affected by choice of T, but the estimates appear to converge in the limit. The set estimates of x^* via this method has the smallest standard deviation, but is not ideal since it is is sensitive to noisy data. In particular, it selects the *first* index at which the histogram exceeds T, which does not always capture the "obvious" position of the cutoff as histogram is generally not monotonic, and in fact generally underestimates the cutoff value. This is especially the case at lower population values, where the data is noisy and the approach to the cutoff is gradual (see the histograms for $N = 100$ in Figure 7). This method also does not take into account the overall shape of the distribution except that it approaches uniform. Methods 2 and 3 attempt to address these issues, but lead to a wider range of values for x^*.

4.1.2 Method 2

Since the integral of the limiting uniform fitness distribution is 1, we can estimate x^* by estimating the height h of the distribution, and then computing $x^* = 1 - h^{-1}$. Moreover, since the limiting height is uniform on $(x^*, 1)$, we can choose any subinterval of $(x^*, 1)$ on which to estimate h; in particular we can choose an interval with an upper bound of x^* as its left endpoint. To avoid the noisy "left

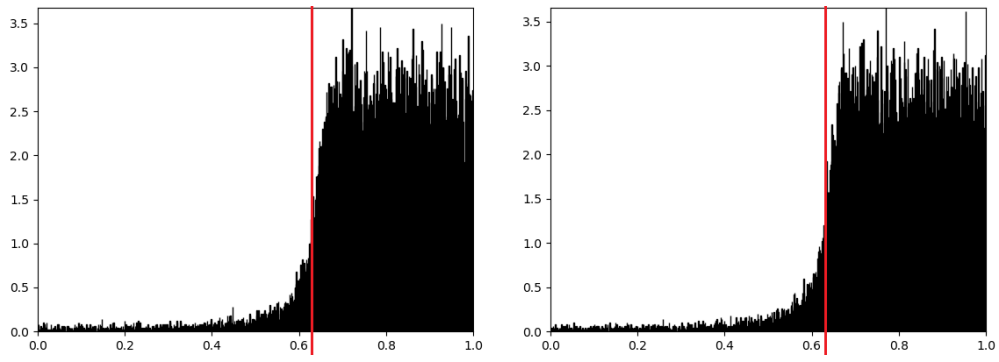

(a) Mersenne: $N = 100$

(b) Xoshiro: $N = 100$

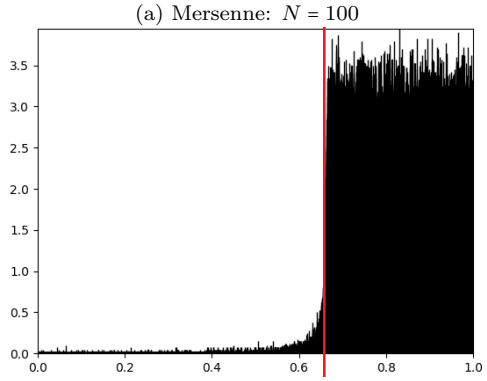

(c) Mersenne: $N = 800$

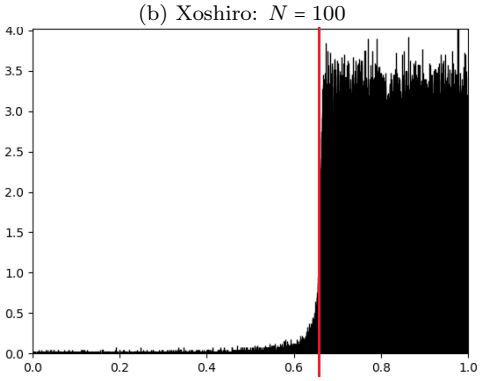

(d) Xoshiro: $N = 800$

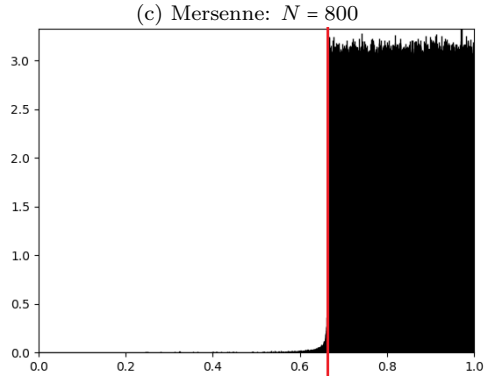

(e) Mersenne: $N = 6400$

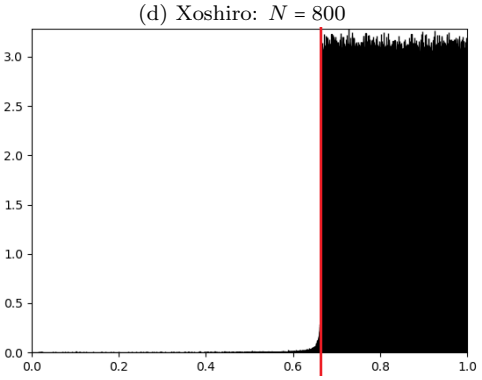

(f) Xoshiro: $N = 6400$

Figure 7: Histograms of fitness values for 500 population samples made after reaching the stationary distribution. The cutoff is distinct at the higher population counts, and is represented in the figure by a red line. Each histogram depicts one of 40 executions (20 per RNG). They are normalized to have area 1.

i	0	1	2	3	4	5	6	7	8
N	100	200	400	800	1600	3200	6400	12800	25600
Method 1									
Mers.									
$\overline{x}_i^*$	0.60653	0.63885	0.65309	0.66033	0.66347	0.66512	0.66598	0.66637	0.66668
s_i	0.00916	0.00265	0.00144	0.00074	0.00025	0.00013	0.00005	0.00004	0.00003
Xosh.									
$\overline{x}_i^*$	0.60193	0.63981	0.65362	0.66031	0.66349	0.66502	0.66596	0.66635	0.66669
s_i	0.01197	0.00332	0.00128	0.00033	0.00024	0.00013	0.00006	0.00002	0.00002
Comb.									
$\overline{x}_i^*$	0.60423	0.63933	0.65335	0.66032	0.66346	0.66506	0.66597	0.66641	0.66668
s_i	0.01091	0.00304	0.00139	0.00057	0.00025	0.00014	0.00006	0.00003	0.00003
Method 2									
Mers.									
$\overline{x}_i^*$	0.61211	0.63368	0.64661	0.65509	0.65967	0.66274	0.66446	0.66557	0.66617
s_i	0.00305	0.00154	0.00089	0.00036	0.00036	0.00015	0.00016	0.00010	0.00012
Xosh.									
$\overline{x}_i^*$	0.61252	0.63400	0.64697	0.65514	0.65977	0.66278	0.66444	0.66555	0.66618
s_i	0.00288	0.00158	0.00065	0.00050	0.00032	0.00024	0.00016	0.00005	0.00009
Comb.									
$\overline{x}_i^*$	0.61231	0.63384	0.64679	0.65511	0.65972	0.66276	0.66445	0.66556	0.66618
s_i	0.00297	0.00157	0.00080	0.00044	0.00035	0.00020	0.00016	0.00008	0.00011

Table 3: The mean and standard deviation (over 20 executions) of the cutoff estimated via Methods 1 and 2, for each population value and for each RNG (Mersenne twister, Xoshiro) and for the combined data (found by pooling data from each RNG before taking the mean and standard deviation). Note that the population values are of the form $N = 100 \cdot 2^i$ for $i \in \{0, 1, 2, 3, 4, 5, 6, 7, 8\}$. Note also that there values do not correspond directly with Figure 1, as the latter values are obtained via the randomized data method described below.

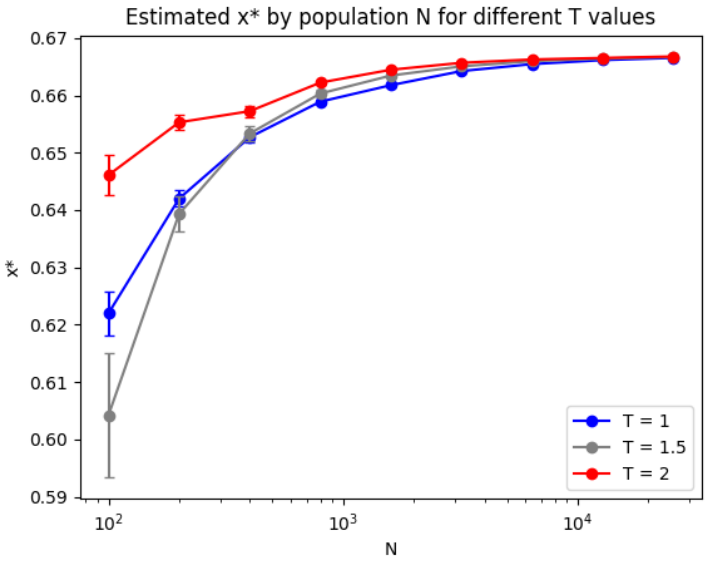

Figure 8: **Method 1** estimates the cutoff by determining the first index at which the histogram exceeds a chosen value T. Because the limiting distribution is singular at x^*, any choice of T will give the same cutoff value in the limit. Estimated values of the cutoff x^* are plotted for different populations N and a range of choices of T. (Note the logarithmic scale of the x-axis.)

edge" of the rectangle, we chose the interval $(0.8, 1)$ and estimate h by simply averaging the height of the histogram on that interval. Observe that this method ignores the fact that a non-zero portion of the distribution lies below the cutoff in every finite empirical fitness histogram. This means that the height of the right-half of the empirical histogram is *lower* than that of a uniform distribution with the same cutoff value, so that the method will tend to underestimate the cutoff. Method 3 below addresses this concern.

4.1.3 Method 3

One may observe (e.g. Figure 7) that for finite N the fitness distribution has some non-zero density in the interval $(0, x^*)$, which appears (at all population levels) to roughly follow a power law. This suggests a density of the form:

$$\rho_N(x) = \begin{cases} \beta_N(\gamma_N - x)^{\alpha_N} & 0 \le x < \gamma_N \\ \frac{1}{1-\gamma_N} & \gamma_N \le x \le 1 \end{cases}$$

for some α_N, β_N and γ_N. Thus, by fitting such a ρ_N to a given histogram, we have the estimate $x^* \approx \gamma_N$. By performing this fit for each trial (at a given population level), we have a set of estimated values of α_N, β_N and γ_N summarized in Table 4. See also Figure 9. Note that for this method we pooled all data at a given population leve (from both RNGs) since the previous methods indicated that the difference between them was minimal and allowed for a greater amount of data.

Modeling the fitness histograms with the scaling density ρ_N clearly exhibits the approach to a uniform distribution (see Figure 11). It also allows for a simple estimate of the proportion of the density lying below the cutoff as $N \to \infty$ (see Figure 12).

N	100	200	400	800	1600	3200	6400	12800	25600
$\overline{\alpha}_N$	-0.48111	-0.53420	-0.59730	-0.66636	-0.57371	-0.61219	-0.65546	-0.75983	-0.81332
s_i	0.05772	0.04334	0.02149	0.02445	0.01894	0.03071	0.04463	0.04704	0.06853
$\overline{\beta}_N$	0.04133	0.02690	0.01591	0.00906	0.00745	0.00473	0.00278	0.00114	0.00065
s_i	0.00848	0.00341	0.00090	0.00083	0.00100	0.00081	0.00069	0.00042	0.00027
$\overline{\gamma}_N$	0.61264	0.63471	0.64756	0.65566	0.65990	0.66303	0.66473	0.66590	0.66644
s_i	0.00312	0.00256	0.00118	0.00074	0.00042	0.00030	0.00027	0.00016	0.00018

Table 4: **Method 3**. The mean and standard deviation of sets of best-fit parameters α_N, β_N, and γ_N for each population level. The curve given by$\rho_N(x) = \beta_N(\gamma_N - x)^{\alpha_N}$ for $x \in (0, \gamma_N)$ models the density of the fitness distribution below the cutoff $x^* \approx \gamma_N$. Above the cutoff the density is the constant $h = (1 - \gamma_N)^{-1}$.

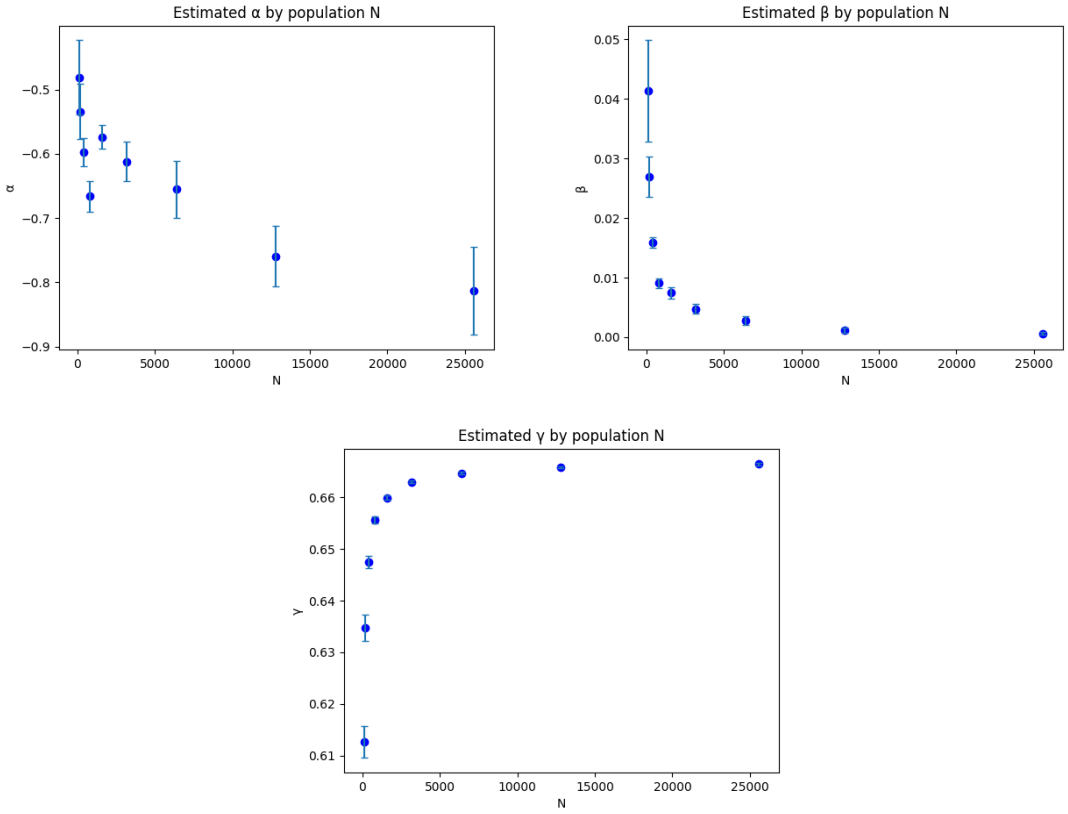

Figure 9: **Method 3.** Estimated parameters α_N, β_N, and γ_N for each population level.

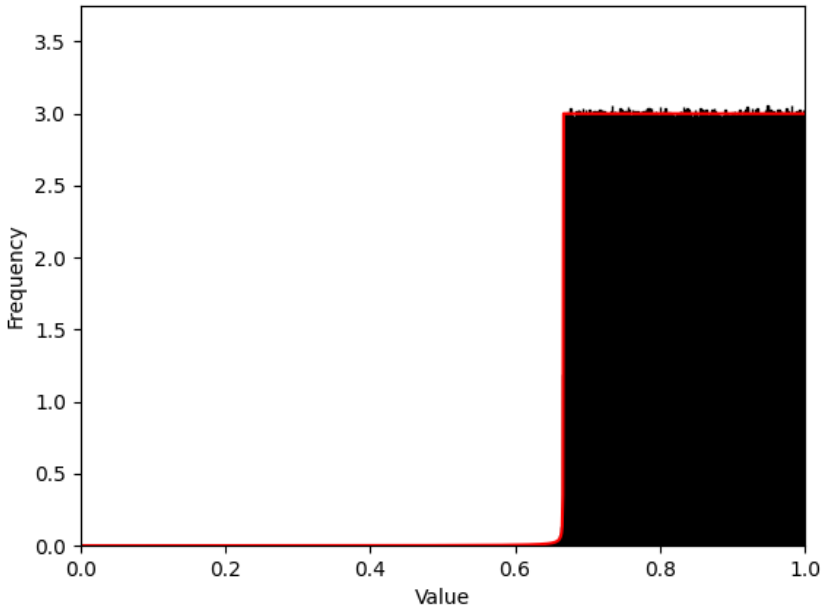

Figure 10: **Method 3.** One fitness histogram at $N = 25600$ with the best-fit curve ρ_N superimposed.

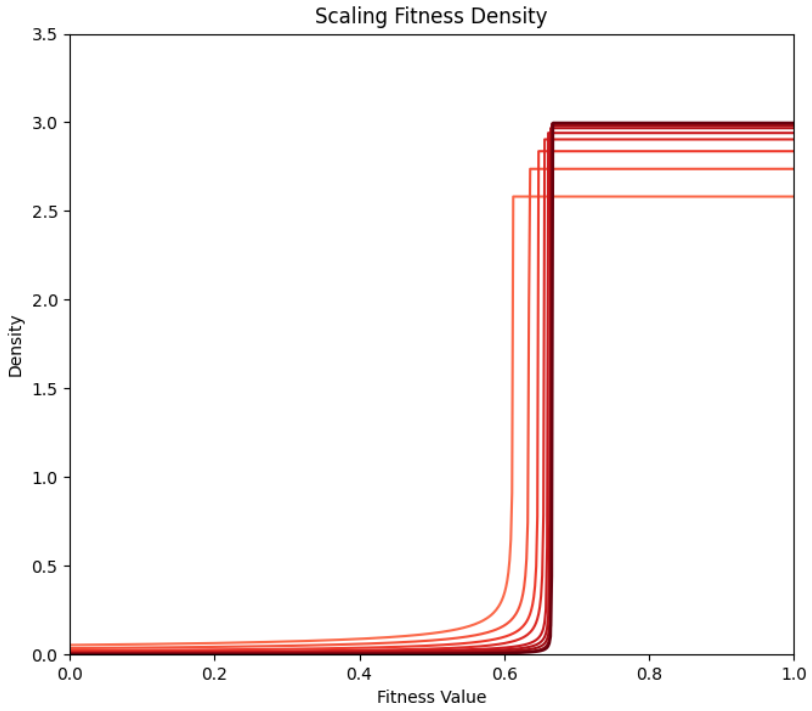

Figure 11: **Method 3.** The range of best-fit curves ρ for each population level N are superimposed, exhibiting a clear approach to a uniform distribution. Note that the maximum value of each density is increasing as N increases.

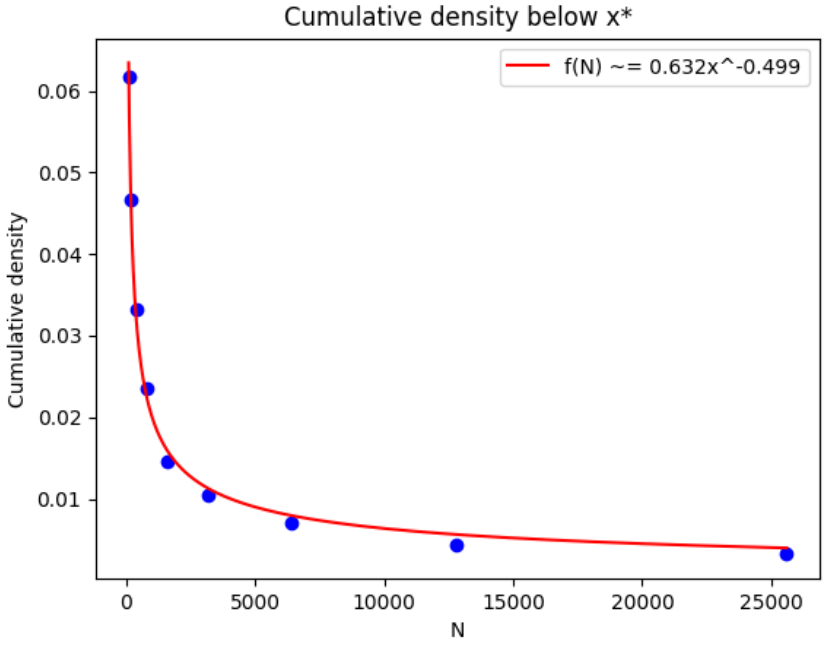

Figure 12: **Method 3.** Estimated cumulative density in the interval $(0, x^*)$ for each population level is determined by numerically integrating the best-fit density curve ρ_N. This quantity vanishes as ρ_N approaches a uniform distribution in the limit $N \to \infty$.

4.2 *Estimating* x^*

Using the estimates for the values of x_N^* determined by each method, we performed a statistical estimation of the cutoff at infinity $x^* = \lim_{N\to\infty} x_N^*$ using maximum likelihood estimation (MLE). Supposing that the values x_N^* follow the function

$$x^*_{100\cdot 2^i} := f(i) = x^* - \kappa\lambda^i\,, \tag{1}$$

we used MLE to estimate the parameters x^*, κ, and λ. In particular, for $i \in \{0, ..., 8\}$, let $\overline{x}_i$ be the mean obtained via histogram and let s_i be the corresponding standard deviation (see Table 3). Then determine x^*, κ and λ that minimize

$$\chi^2(x^*, \kappa, \lambda) = \sum_{n=0}^{8} \frac{(\overline{x}_i - f(i))^2}{{s_i}^2}\,,$$

where $f(i)$ is given by (1). We minimized χ^2 via gradient method with a variable step[7]. This resulted in the estimated values for x^*, κ, and λ, seen in Table 5, for each RNG.

We take the x^*, κ, and λ associated with the combined data to be our best initial estimates. Beginning with these values, we determine our final estimates via the randomized data method described below.

4.3 *Estimating errors on parameters*

Having obtained an estimate for the cutoff, we estimated the error of our estimate using the following randomized data method. Initially, for each population level, and each RNG, we obtained an empirical

[7]In particular, we performed the backtracking line search method to determine the step size.

Source	x^*	λ	κ	χ^2
Method 1				
Mersenne	0.66688	0.50525	0.05422	3.99643
Xoshiro	0.66697	0.53743	0.04442	13.72710
Combined	0.66690	0.51008	0.05242	2.62146
Method 2				
Mersenne	0.66717	0.60361	0.05547	0.53577
Xoshiro	0.66716	0.60421	0.05500	0.26683
Combined	0.66717	0.60357	0.05563	0.41982
Method 3				
Combined	0.66748	0.60659	0.05441	0.72618

Table 5: Initial optimized parameters minimizing the χ^2 function, given the data in Table 3. The minimum χ^2 value attained via these parameters is reported. These constitute a single set of optimized parameters, whereas the randomized data method of Section 4.3 provides a range of values for these parameters (see Table 6).

Source	Mean x^*	$\pm$	Mean λ	$\pm$	Mean κ	$\pm$	Mean ν	$\pm$
Method 1								
Mersenne	0.66689	0.00004	0.51075	0.00631	0.05194	0.00284	0.96930	0.01771
Xoshiro	0.66694	0.00004	0.53091	0.01020	0.04597	0.00265	0.91346	0.02744
Combined	0.66688	0.00003	0.50758	0.00860	0.05393	0.00291	0.97830	0.02425
Method 2								
Mersenne	0.66717	0.00014	0.60166	0.00770	0.05609	0.00172	0.73298	0.01834
Xoshiro	0.66715	0.00014	0.60308	0.00846	0.05536	0.00135	0.72958	0.02010
Combined	0.66717	0.00010	0.60690	0.00713	0.05444	0.00173	0.72048	0.01685
Method 3								
Combined	0.66747	0.00025	0.60799	0.01142	0.05355	0.00176	0.71788	0.02685

Table 6: Mean cutoff values and estimated standard deviation obtained via the randomized data method, for each RNG. Mean and standard deviation of associated λ, κ, and ν are also reported. To obtain the "combined" results, we pooled together empirical cutoff data from both RNGs before performing the randomization procedure. As before, we report the "Combined" data for our best estimates.

cutoff value $\overline{x}_i^*$ as a mean over 20 executions, and also obtained a standard deviation s_i. Supposing that these data were drawn from a normal distribution $\mathcal{N}$ with mean $\overline{x}_i^*$ and standard deviation s_i, we drew 10 new samples from $\mathcal{N}$ and performed the same MLE process described above, beginning with these artificial data. This process provided larger set of possible cutoff values, whose mean and standard deviation we report in Table 6. We take these means to be our best estimates for the Bak-Sneppen cutoff given by each method. We also report the mean and standard deviation of the associated values of λ, κ, and ν. See below for a discussion of ν, as well as Figures 13 and 14 illustrating models for $x^* - x_N^*$ fit with these mean parameters.

4.4 *Estimating the exponent ν*

To estimate ν in

$$x^* - x_N^* \propto N^{-\nu},$$

we need to rewrite this equation in terms of the parameters used so far. Recall that $x^*_{100\cdot 2^i}$ is written as $f(i)$. So from (1), while noting that $i = \log_2(N/100)$, we obtain

$$x^* - x^*_N = \kappa\,\lambda^i = \kappa\,\lambda^{\log_2 N - \log_2 100} = \left(\kappa\,\lambda^{-\log_2 100}\right)\,\lambda^{\log_2 N} \propto N^{\ln\lambda/\ln 2}\,,$$

since $\log_2 N = \ln N/\ln 2$. Thus we obtain

$$\nu = -\ln\lambda/\ln 2\,.$$

To get an idea, take the first two values for λ in Table 5. This gives $\nu = 0.985$ and $\nu = 0.896$. Thus ν is particularly sensitive to variations in λ. We found an estimated range of values for κ and λ, and the corresponding range of values for ν, as reported in Table 6.

5 Conclusion

We summarize our results in Table 7 (see also Figure 1).

Source	Estimated x^*	±	Minimum	Maximum
Grassberger [5]	0.66702	0.00008	0.66694	0.66710
Paczuski [13]	0.66702	0.00004	0.66698	0.66706
Garcia [3]	0.66720	0.00020	0.66700	0.66740
Method 1	0.66688	0.00004	0.66684	0.66692
Method 2	0.66717	0.00010	0.66707	0.66726
Method 3	0.66747	0.00025	0.66722	0.66772

Table 7: Summary of our simulation results compared to cutoff values previously estimated. The minimum and maximum values (based on the reported error) are listed for ease of comparison.

Broadly, these results agree with the values previously obtained in the literature. As our simulations did not make use of the scaling assumptions found in e.g. [13], this suggests that these assumptions are reasonable and, in particular, that any error they introduce in the cutoff value cannot be much greater than $\approx 0.66740 - 0.66684 = 0.00056$ (the difference between the maximum estimated value under scaling assumptions and the minimum estimated value under direct simulation).

Method 1, as expected, provides an underestimate of the cutoff, illustrated most dramatically by Figure 13, in which the underestimate at the lowest population values skews ν, the key parameter on the overall fit of these data to a curve $x^* - x^*_N \propto N^{-\nu}$. This, along with the fact that it is significantly lower than reported in the literature indicates that Method 1 is not ideal for measuring the cutoff, and that the value of ν it provides should not be given much weight. However, Method 1 did provide the narrowest range of possible values, suggesting that an appropriately modified version could provide the most accurate estimates of the true cutoff value.

The estimates provided by Methods 2 and 3, while less precise than Method 1, do generally agree with the literature and take into account more information about the shape of the distribution. Method 3 in particular closely models the density on both sides of the cutoff and suggests a deeper exploration of the scaling properties of the fitness distribution. Both methods give a similar value for $\nu \approx 0.72$, which is notably lower than previously measured (see [3]). The cutoff value given by Method 2 is lower than the value given by Method 3, likely because of its discussed tendency to underestimate the height of the true distribution (and hence the value $x^* = 1 - h^{-1}$).

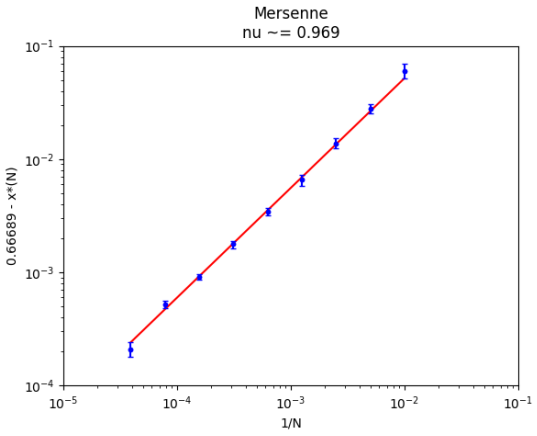

(a) Method 1, Mersenne Twister

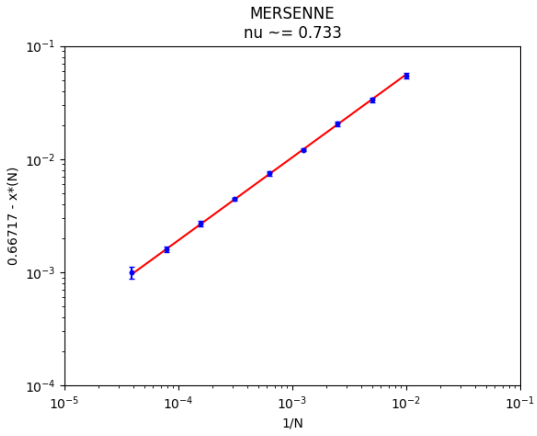

(b) Method 2, Mersenne Twister

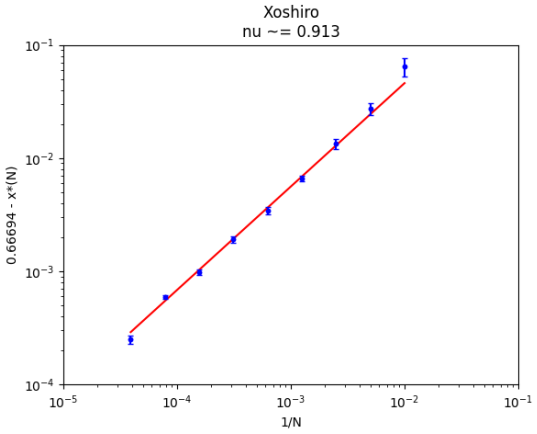

(c) Method 1, Xoshiro

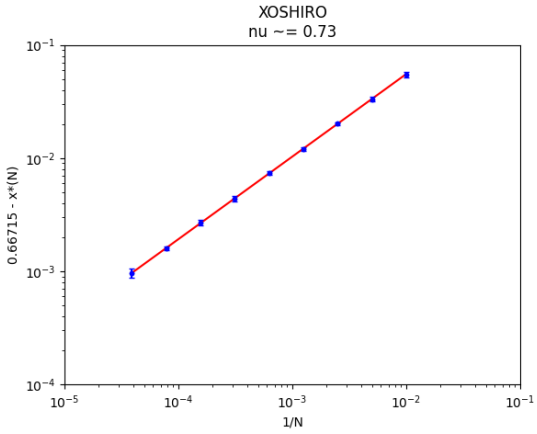

(d) Method 2, Xoshiro

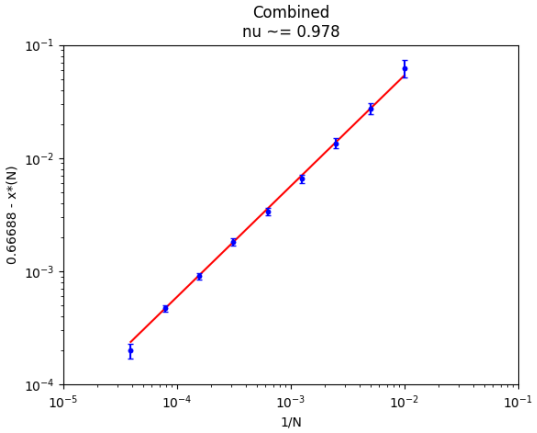

(e) Method 1, Combined

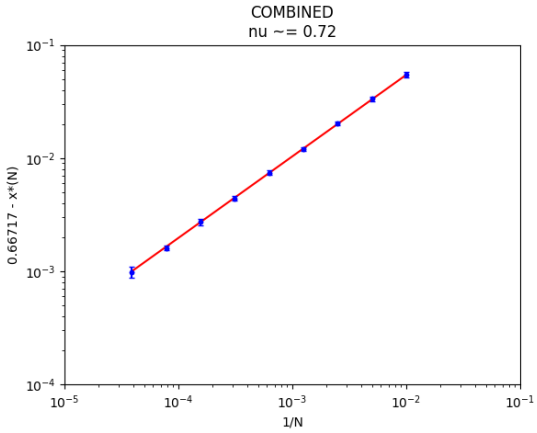

(f) Method 2, Combined

Figure 13: Reformulating the model $x^*_{100\cdot 2^i} = f(i) = x^* - \kappa\lambda^i$ as a function of $\frac{1}{N}$, we can write $x^* - x^*_N = \left(\kappa\,\lambda^{-\log_2 100}\right) N^{-\nu}$, where $\nu = -\ln\lambda/\ln 2$. The figures show both the original x^*_N data alongside the model, using the mean parameters found in Table 6. Note that ν is the slope of the line, and is smaller than previously reported (e.g. [3] gives $\nu \approx 1.4$).

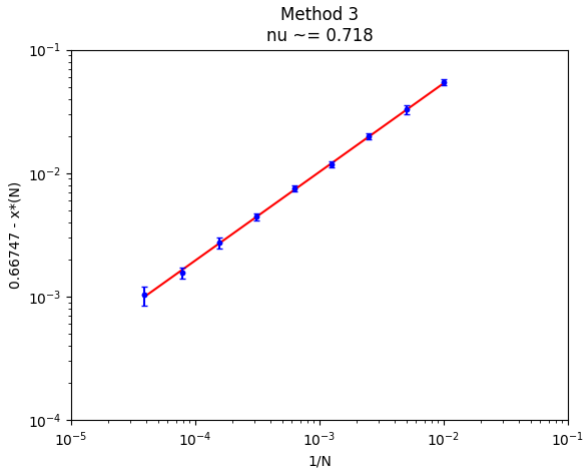

Figure 14: The fit of $x^* - x_N^* = \left(\kappa\, \lambda^{-\log_2 100}\right) N^{-\nu}$ to the cutoff values x_N^* obtained via Method 3. Note that the value of ν approximately agrees with the value found in Method 2.

Taking the value $x^* = 0.66747 \pm 0.00025$ obtained by Method 3 to be our best estimate, we note that it is significantly larger that other values reported in the literature. This suggests that a deeper investigation of the scaling law approach is warranted in order to more precisely determine the true value of x^*.

6 Data availability statement

The data that support the findings of this study are available from the corresponding author, Cameron Fish, upon request. The simulation is written in C and the subsequent statistical analysis was performed with Python. The code for both can be found at `https://github.com/camafish/Bak-Sneppen`.

Acknowledgement. We are grateful to Javier Prieto and Daniel Taylor-Rodriguez for their generous help with the statistics involved in this work.

References

[1] Per Bak and Kim Sneppen. Punctuated equilibrium and criticality in a simple model of evolution. *Physical Review Letters*, 71(24):4083–4086, 1993.

[2] Jan de Boer, A. D. Jackson, and Tilo Wettig. Criticality in simple models of evolution. *Phys. Rev. E*, 51:1059–1074, Feb 1995. `https://link.aps.org/doi/10.1103/PhysRevE.51.1059`.

[3] G. J. M. Garcia and R. Dickman. On the thresholds, probability densities, and critical exponents of bak-sneppen-like models. *Physica A*, 342:164–170, 2004.

[4] Stephen Jay Gould and Niles Eldredge. Punctuated equilibria: The tempo and mode of evolution reconsidered. *Paleobiology*, 3(2):115–151, 1977.

[5] P. Grassberger. The bak-sneppen model for punctuated evolution. *Physics Letters A 200*, pages 277–282, 1995.

[6] Michael Grinfeld, Philip A. Knight, and Andrew R. Wade. Bak-sneppen-type models and rank-driven processes. *Phys. Rev. E*, 84:041–124, Oct 2011. https://link.aps.org/doi/10.1103/PhysRevE.84.041124.

[7] Michael Grinfeld, Philip A. Knight, and Andrew R. Wade. Rank-driven markov processes. *Journal of Statistical Physics*, 146(2):378–407, Oct 2011.

[8] William Kahan. Lecture notes on the status of ieee standard 754 for binary floating-point arithmetic, October 1997. https://people.eecs.berkeley.edu/~wkahan/ieee754status/IEEE754.PDF.

[9] Makoto Matsumoto and Takuji Nishimura. Mersenne twister: A 623-dimensionally equidistributed uniform pseudo-random number generator. *ACM Trans. Model. Comput. Simul.*, 8(1):3–30, January 1998. https://doi.org/10.1145/272991.272995.

[10] R. Meester and Dmitri Znamenski. Limit behavior of the bak-sneppen evolution model. *Annals of Probability*, 31:1986–2002, 2003.

[11] Ronal Meester and Dmitri Znamenski. Critical thresholds and the limit distribution in the bak-sneppen model. *Communications in Mathematical Physics*, 246:63–86, 2004. https://doi.org/10.1007/s00220-004-1044-4.

[12] M.S. Nikulin. Cramér-von mises test., 2011. https://encyclopediaofmath.org/index.php?title=Cramer-von_Mises_test&oldid=11734.

[13] M. Paczuski, S. Maslov, and P. Bak. Avalanche dynamics in evolution, growth, and depinning models. *Physical Review E*, 53:414–443, 1996.

[14] J. J. P. Veerman and Francisco J. Prieto. On rank driven dynamical systems. *Journal of Statistical Physics*, 156:455–472, 2014.

[15] Sebastiano Vigna and David Blackman. xoshiro / xoroshiro generators and the prng shootout. https://prng.di.unimi.it/.